

# RSC Advances



This is an *Accepted Manuscript*, which has been through the Royal Society of Chemistry peer review process and has been accepted for publication.

*Accepted Manuscripts* are published online shortly after acceptance, before technical editing, formatting and proof reading. Using this free service, authors can make their results available to the community, in citable form, before we publish the edited article. This *Accepted Manuscript* will be replaced by the edited, formatted and paginated article as soon as this is available.

You can find more information about *Accepted Manuscripts* in the [Information for Authors](#).

Please note that technical editing may introduce minor changes to the text and/or graphics, which may alter content. The journal's standard [Terms & Conditions](#) and the [Ethical guidelines](#) still apply. In no event shall the Royal Society of Chemistry be held responsible for any errors or omissions in this *Accepted Manuscript* or any consequences arising from the use of any information it contains.

# Polyamine-assisted hydrothermal synthesis of bimetallic Pd<sub>1</sub>Cu<sub>3</sub> multipods and their high catalytic ability in 4-nitrophenol reduction

Cite this: DOI: 10.1039/x0xx00000x

Xiaoyu Qiu,<sup>‡</sup> Ruopeng Zhao,<sup>‡</sup> Yanan Li, Yawen Tang,<sup>\*</sup> Dongmei Sun, Shaohua Wei,<sup>\*</sup> and Tianhong Lu

Received 00th January 2012,  
Accepted 00th January 2012

DOI: 10.1039/x0xx00000x

www.rsc.org/

**Bimetallic Pd<sub>1</sub>Cu<sub>3</sub> multipod nanocrystals (Pd<sub>1</sub>Cu<sub>3</sub>-MNCs) are synthesized by a facile hydrothermal method. The catalytic reduction of Cu<sup>II</sup> by Pd crystal nuclei is critical for the formation of Pd<sub>1</sub>Cu<sub>3</sub>-MNCs. Pd<sub>1</sub>Cu<sub>3</sub>-MNCs show remarkably enhanced catalytic activity for the hydrogenation reduction of nitro functional groups compared to the commercial Pd black.**

Pd-based bimetallic nanocrystals have been intensively explored as effectively catalytic materials in the field of organic synthesis and electrocatalysis. Compared to single-component Pd nanocrystals, Pd-based bimetallic nanocrystals generally displayed superior catalytic/electrocatalytic activities because of the geometric effect, electronic effect and synergistic effect between different components.<sup>1-5</sup> Meanwhile, the morphologies of Pd nanocrystals affected their catalytic/electrocatalytic activities and stability because of structure effect. For example, highly branched Pd multipod nanocrystals with structural anisotropy exhibited remarkably improved electrocatalytic/catalytic activities and stabilities owing to high density of low-coordinated atoms (such as steps, kinks, terraces, islands and vacancies) and particular self-supported structure that could effectively suppresses Ostwald ripening or grain growth.<sup>6-10</sup>

Recently, Pd-Cu alloy nanocrystals have been widely used as effective catalysts for the methanol oxidation reaction, nitrate electroreduction, oxygen reduction reaction, formic acid oxidation reaction, etc., which not only exhibited higher catalytic activities compared with monometallic Pd nanocrystals but also reduced the cost significantly.<sup>3, 11-16</sup> Nielsenite (Pd<sub>1</sub>Cu<sub>3</sub>), a palladium-group bimetallic mineral material, was discovered and named by Nielsen.<sup>17</sup> Although various Pd-Cu alloy nanocrystals with various elemental compositions have been synthesized, Pd<sub>1</sub>Cu<sub>3</sub> nanocrystals were rarely synthesized and investigated. Maybe, the different

reduction kinetics of Pd<sup>II</sup> and Cu<sup>II</sup> precursors resulted in difficulty in the formation of Pd-Cu alloy because of their distinct standard reduction potentials (Pd<sup>2+</sup>/Pd<sup>0</sup>: 0.915 V vs. RHE; Cu<sup>2+</sup>/Cu<sup>0</sup>: 0.342 V vs. RHE). In this work, we demonstrated a one-pot hydrothermal method to synthesize bimetallic Pd<sub>1</sub>Cu<sub>3</sub> multipod nanocrystals (Pd<sub>1</sub>Cu<sub>3</sub>-MNCs) based on catalytic growth mechanism. To the best of our knowledge, there is no report on the synthesis of bimetallic Pd<sub>1</sub>Cu<sub>3</sub> nanomaterials. The as-prepared Pd<sub>1</sub>Cu<sub>3</sub>-MNCs exhibited remarkably enhanced catalytic activity for the hydrogenation reduction of nitro functional groups over commercially available Pd black.

In a typical synthesis, Pd<sub>1</sub>Cu<sub>3</sub>-MNCs were prepared by reducing PdCl<sub>2</sub> and CuCl<sub>2</sub> precursors with HCHO in aqueous PAH solution at 120 °C for 6 h (see Experimental section for details). The morphology and size of products were firstly investigated by transmission electron microscopy (TEM). Tetrapods, pentapods, hexapods and other multipods are observed from the same mixture (Fig. 1A-B). The particle size of whole multipods is 30±10 nm whereas the length of each pod is 15±5 nm. Energy dispersive X-ray spectroscopy (EDX) analysis indicates that the average composition of multipods is Pd<sub>27</sub>Cu<sub>73</sub> (Fig. 1C), which is consistent with the PdCl<sub>2</sub>/CuCl<sub>2</sub> feeding ratio. In XPS spectrum of Pd 3d, the most intense doublet of peaks (3d<sub>5/2</sub> = 334.98 eV; 3d<sub>3/2</sub> = 340.22 eV) are ascribed to the metallic Pd, while the weaker doublet of peaks (3d<sub>5/2</sub> = 336.35 eV; 3d<sub>3/2</sub> = 341.98 eV) are assigned to PdO (Fig. 1D). By measuring the relative peak areas, the percentage of metallic Pd<sup>0</sup> is calculated to be 93.1%. Meanwhile, XPS spectrum of Cu 2p displays a doublet of peaks (2p<sub>3/2</sub>=932.4 eV; 2p<sub>1/2</sub>=952.4 eV), which is indicative of metallic Cu (Fig. 1F). Thus, XPS measurements demonstrate that Pd<sup>II</sup> and Cu<sup>II</sup> precursors are reduced successfully. X-ray diffraction (XRD) pattern demonstrates that Pd<sub>1</sub>Cu<sub>3</sub> multipods can be identified as face-centered cubic (*fcc*) structure (Figure 1G). The diffraction peaks of Pd<sub>1</sub>Cu<sub>3</sub> multipods are located

between those of pure *fcc* Pd (PDF#46-1043) and Cu (PDF#04-0836) crystal phases, indicating that Pd<sub>1</sub>Cu<sub>3</sub> multipods are indeed alloys. The lattice parameter value (*a*) of Pd<sub>1</sub>Cu<sub>3</sub> multipods is calculated to be 0.3783 nm based on Scherrer's formula, in consistent with that of Pd<sub>1</sub>Cu<sub>3</sub> intermetallic mineral material reported by McDonald,<sup>17</sup> indicating that Pd<sub>1</sub>Cu<sub>3</sub> multipods may be intermetallic compound.

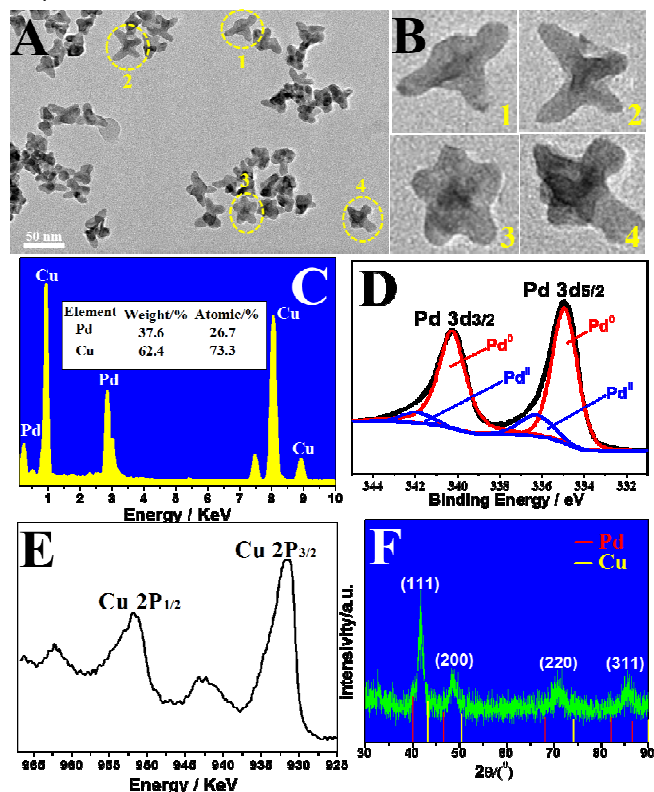


Fig. 1 (A) Representative large-area TEM images of Pd<sub>1</sub>Cu<sub>3</sub>-MNCs. (B) Magnified TEM images taken from regions marked by squares in Figure 1A. (C) EDX spectrum of Pd<sub>1</sub>Cu<sub>3</sub>-MNCs. (D) XPS spectrum of Pd<sub>1</sub>Cu<sub>3</sub>-MNCs in Pd 3d region. (E) XPS spectrum of Pd<sub>1</sub>Cu<sub>3</sub>-MNCs in Cu 2p region. (F) XRD pattern of Pd<sub>1</sub>Cu<sub>3</sub>-MNCs.

The detailed structure of Pd<sub>1</sub>Cu<sub>3</sub>-MNCs was investigated by selecting bimetallic Pd<sub>1</sub>Cu<sub>3</sub> tetrapod as representative sample. As observed, Pd<sub>1</sub>Cu<sub>3</sub> tetrapods in TEM image have four obvious pods with ca. 15 nm length (Fig. 2A). The fringes with a interplanar spacing of 0.185 nm are observed at most region on a pod (Fig. 2B), very close to the {200} interplanar spacing of the *fcc* bimetallic Pd<sub>1</sub>Cu<sub>3</sub> material (0.186 nm).<sup>17</sup> Selected-area electron diffraction (SAED) image demonstrates that bimetallic Pd<sub>1</sub>Cu<sub>3</sub> tetrapods have a polycrystalline structure (Fig. 2C), which is typical characteristic of metal multipods. High-angle annular dark-field scanning TEM (HAADF-STEM) image reveals that bimetallic Pd<sub>1</sub>Cu<sub>3</sub> tetrapods possess the same luminance (Fig. 2D), indicating bimetallic Pd<sub>1</sub>Cu<sub>3</sub> tetrapods have an alloy structure rather than a core-shell structure. EDX elemental mapping (Fig. 2E) and EDX line scanning profile (Fig. 2F) clearly show the distribution of Pd atoms is completely consistent with that of Cu atoms, confirming an alloy structure.

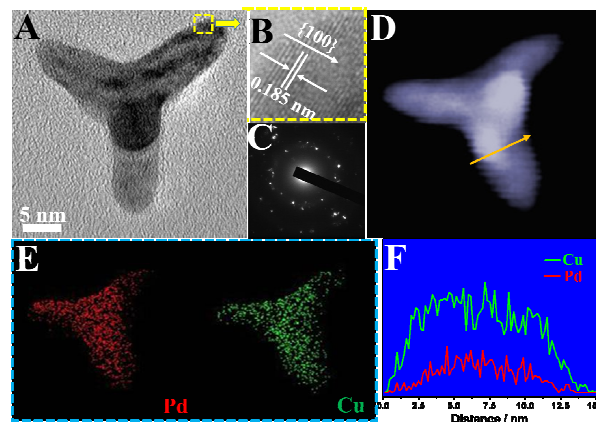


Fig. 2 (A) Typical TEM image of Pd<sub>1</sub>Cu<sub>3</sub>-MNCs. (B) The magnified TEM images recorded from region marked by squares in Figure 2A. (C) SAED pattern of bimetallic Pd<sub>1</sub>Cu<sub>3</sub> tetrapods shown in Figure 2A. (D) HAADF-STEM image of bimetallic Pd<sub>1</sub>Cu<sub>3</sub> tetrapods. (E) EDX elemental mapping patterns of bimetallic Pd<sub>1</sub>Cu<sub>3</sub> tetrapods shown in Figure 2D. (F) EDX line scanning profiles of bimetallic Pd<sub>1</sub>Cu<sub>3</sub> tetrapods shown in Figure 2D.

The high-quality noble metal nanocrystals with especial shape generally are achieved by kinetically controlled synthesis (*i.e.*, slow reduction rate). PAH with a large number of primary amine groups has excellent coordination capability for metal ion.<sup>18, 19</sup> As observed, a lot of red PdO•H<sub>2</sub>O and blue Cu(OH)<sub>2</sub> precipitates generate immediately once adjusting pH values of single-component PdCl<sub>2</sub> and CuCl<sub>2</sub> solutions to 10.0, respectively (Fig. 3A). In contrast, in the presence of PAH, the colorless PAH-Pd<sup>II</sup> and blue PAH-Cu<sup>I</sup> complexes solution can be facily obtained at pH 10.0 via coordination interaction, respectively (Fig. 3B).

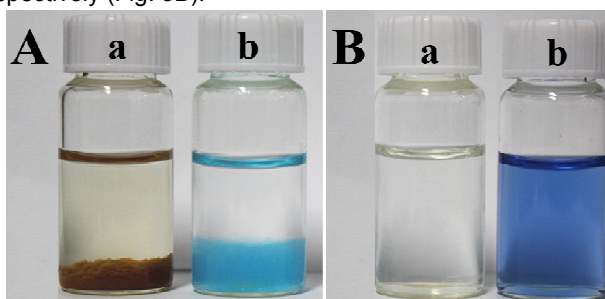


Fig. 3 (A) Photographs of (a) red PdO•H<sub>2</sub>O and (b) blue Cu(OH)<sub>2</sub> precipitations obtained by adjusting pH values of single-component PdCl<sub>2</sub> and CuCl<sub>2</sub> solutions to 10.0, respectively. (B) Photograph of (a) colorless PAH-Pd<sup>II</sup> and (b) blue PAH-Cu<sup>I</sup> complex solutions obtained by adjusting pH values of PdCl<sub>2</sub>/PAH and CuCl<sub>2</sub>/PAH mixture solutions to 10.0, respectively.

The generations of PAH-Pd<sup>II</sup> and PAH-Cu<sup>I</sup> complexes are expected to effectively decrease the reduction potential of Pd<sup>II</sup> and Cu<sup>II</sup> species. As confirmed, the reduction peak potentials of PAH-Pd<sup>II</sup> and PAH-Cu<sup>II</sup> complexes show 0.54 V and 0.1 V shifts to more negative potential compared with the single-component PdCl<sub>2</sub> and CuCl<sub>2</sub> solutions, respectively (Fig. 4A-B), which facilitates the formation of high-quality Pd-Cu bimetallic nanocrystals because of the slow reduction rate. TEM images show the reaction is completed at 4 h (Fig. S1, ESI†), confirming the slow reduction rate. According to thermodynamical view, the Pd@Cu core-shell nanocrystals should be predominant products because the reduction potential for Cu<sup>II</sup>/Cu<sup>0</sup> is much lower than that of Pd<sup>II</sup>/Pd<sup>0</sup> pairs

under the present experimental conditions. Surprisingly, Pd<sub>1</sub>Cu<sub>3</sub>-MNCs are achieved in the present synthesis. Indeed, the single-component Cu<sup>II</sup> precursor can't be reduced under the present experimental conditions, indicating that the reduction of Cu<sup>II</sup> ion is facilitated by the preformed Pd crystal nuclei. It is well known that Cu can take place underpotential deposition (UPD, a phenomenon of electrodeposition of a metal ion at a potential less negative than the Nernst equilibrium potential for the reduction of this metal) on Pd surface.<sup>20, 21</sup> Thus, catalytic reduction of Cu<sup>II</sup> ion by Pd crystal nuclei can be ascribed to UPD effect because of the change in thermodynamics energy. Meanwhile, similar to case of Pd-Ni and Pt-Ni alloy nanocrystals,<sup>22-25</sup> the deposited surface Cu atoms are then mixed with Pd atoms through an interdiffusion process because of thermal energy, accompanying the simultaneously direct reduction of Pd<sup>II</sup> precursor, and bimetallic Pd<sub>1</sub>Cu<sub>3</sub> alloy nanocrystals ultimately forms.

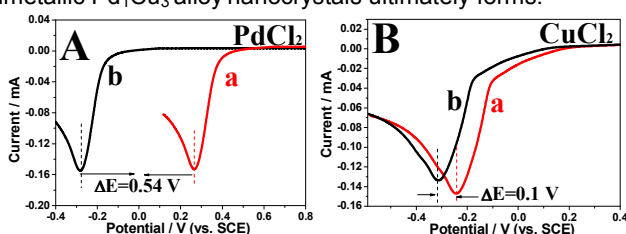


Fig. 4 (A) Linear sweeping voltammograms of N<sub>2</sub>-saturated (a) 0.005 M PdCl<sub>2</sub> + 0.5 M KCl solution and (b) 0.005 M PdCl<sub>2</sub> + 0.05 M PAH + 0.5 M KCl solution at the glassy carbon electrode at a scan rate of 100 mV s<sup>-1</sup> at pH 3.0, respectively. (B) Linear sweeping voltammograms of N<sub>2</sub>-saturated (a) 0.005 M CuCl<sub>2</sub> + 0.5 M KCl solution and (b) 0.005 M CuCl<sub>2</sub> + 0.05 M PAH + 0.5 M KCl solution at the glassy carbon electrode at a scan rate of 100 mV s<sup>-1</sup> at pH 3.0, respectively.

The formation of Pd<sub>1</sub>Cu<sub>3</sub>-MNCs depends on the experimental parameters, including reaction temperature and the feeding ratio of precursors. When reaction temperature fixed at 100 °C, both PAH-Pd<sup>II</sup> and PAH-Cu<sup>II</sup> complexes couldn't be reduced. Our previous work indicated the Pd icosahedra could be obtained when single-component Pd<sup>II</sup> precursor was used.<sup>26</sup> When the feeding ratio of Pd<sup>II</sup>/Cu<sup>II</sup> precursors was fixed at 1:1, only Pd<sub>1</sub>Cu<sub>1</sub> nanoflowers were obtained (Fig. S2, ESI†). These facts indicate the addition of high-content Cu<sup>II</sup> precursor favors the formation of bimetallic Pd-Cu multipods. During the synthesis, the adsorption of Cu<sup>II</sup> on the surface of the preformed Pd crystal nuclei may change the growth direction of Pd crystal nuclei. Meanwhile, it is clear that the dissolved O<sub>2</sub> can result in the selective oxidative etching of Cu atoms on the preformed noble metal crystal nuclei surface.<sup>27</sup> Thus, Pd-Cu bimetallic nanocrystals with higher Cu content are more vulnerable to the selective oxidative etching, which facilitates the formation of multipod nanocrystals.

It is clear that the reduction of 4-nitrophenol (4-NP) by NaBH<sub>4</sub> occurred directly on the metallic surface. Therefore, the reduction of 4-NP had become one of the model reactions for evaluating the catalytic activity of noble metal nanomaterials.<sup>28-30</sup> The catalytic mechanism can be explained as follows. 4-NP is electrophilic and BH<sub>4</sub><sup>-</sup> is nucleophilic with respect to noble metal nanomaterials. The nucleophile BH<sub>4</sub><sup>-</sup>

can donate electrons to noble metal nanomaterials, and the electrophile 4-NP can capture electrons from the noble metal nanomaterials. Thus, noble metal nanomaterials can serve as catalytic electron relays for the 4-NP reduction in a NaBH<sub>4</sub> solution. The reduction process of 4-NP was monitored using time-resolved UV-vis. Upon the introduction of the Pd<sub>1</sub>Cu<sub>3</sub>-MNCs into the reaction solution, the peak of 4-NP at 400 nm decreases rapidly with time, accompanying with the gradual emergence of a new peak at 300 nm corresponding to the formation of 4-aminophenol (Fig. 5A). After 19 min, the peak of 4-NP at 400 nm completely vanishes, indicating the conversion of 4-NP is nearly 100%. For comparison, the catalytic activities of the commercial Pd black and for the 4-NP reduction were also investigated under same experimental conditions. As observed, the reduction of 4-NP to 4-AP is finished within 34 min using the commercial Pd black as catalyst (Fig. 5B), respectively Reaction rate constant  $\kappa$  is calculated from the slope of the linear section of the plots of  $\ln(C_t/C_0)$  versus  $t$  (inserts in Fig. 5A-B). Compared with the commercial Pd black ( $\kappa$ : 0.1 min<sup>-1</sup>), Pd<sub>1</sub>Cu<sub>3</sub>-MNCs exhibit improved catalytic activity for the 4-AP reduction ( $\kappa$ : 0.174 min<sup>-1</sup>). The improved catalytic activity of Pd<sub>1</sub>Cu<sub>3</sub>-MNCs may originate from the following reasons: (i) Metal multipods generally have abundant defect atoms with low-coordination number, which is highly active for catalytic reaction. (ii) Similar to the case of other alloy,<sup>31</sup> synergistic effect between Pd and Cu atoms (such as electronic effect and geometric effect) also contribute to the enhancement in catalytic activity. Under the same total mass conditions, the catalytic activity of the Pd<sub>1</sub>Cu<sub>3</sub>-MNCs with low Pd content is superior to Pd<sub>1</sub>Cu<sub>1</sub> nanoflowers with high Pd content (Fig. S3, ESI†), further exhibiting Pd<sub>1</sub>Cu<sub>3</sub>-MNCs have wide actual application perspective.

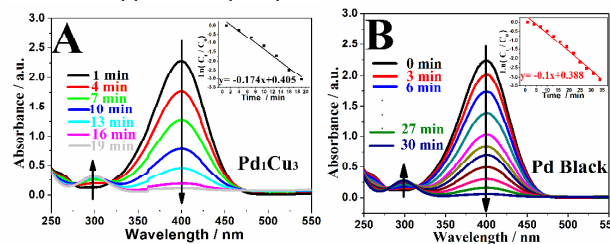


Fig. 5 UV-vis spectra for successive reduction of 4-NP with NaBH<sub>4</sub> using (A) Pd<sub>1</sub>Cu<sub>3</sub>-MNCs and (B) commercial Pd black as catalysts at 3 min intervals. Inserts in A-B: the relationship between  $\ln(C_t/C_0)$  and reaction time ( $t$ ), where in the ratio of the 4-NP concentration ( $C_t$  at time  $t$ ) to its initial value  $C_0$  were directly given by the relative intensity of the respective absorbance  $A_t/A_0$ .

In summary, we reported a simple and green co-chemical reduction route to synthesize Pd<sub>1</sub>Cu<sub>3</sub>-MNCs in aqueous PAH solution. The formation of bimetallic Pd<sub>1</sub>Cu<sub>3</sub> nanocrystals was attributed to the catalytic growth mechanism, which was supported by the fact that Cu<sup>II</sup> ion couldn't be solely reduced under the same experimental conditions. In nature, the multipod morphology and high Cu content of Pd<sub>1</sub>Cu<sub>3</sub>-MNCs were favourable for providing high surface area, enhancing catalytic activity, and reducing the Pd consumption. Indeed, Pd<sub>1</sub>Cu<sub>3</sub>-MNCs exhibited higher catalytic activity for the reduction of 4-NP than the commercial Pd black, indicating that Pd<sub>1</sub>Cu<sub>3</sub>-MNCs might have wide potential applications in

water-based heterogeneous catalytic systems.

### Acknowledgment

The authors are grateful for the financial support of NSFC (21376122 and 21273116), United Fund of NSFC and Yunnan Province (U1137602), Industry-Academia Cooperation Innovation Fund Project of Jiangsu Province (BY2012001), the Natural Science Foundation of Jiangsu Higher Education Institutions of China (No. 13KJA1500030), Postgraduate Research and Innovation Project in Jiangsu Province (CXLX13-369), and a project funded by the Priority Academic Program Development of Jiangsu Higher Education Institutions.

### Notes and references

*Jiangsu Key Laboratory of New Power Batteries, Jiangsu Collaborative Innovation Center of Biomedical Functional Materials, School of Chemistry and Materials Science, Nanjing Normal University Nanjing 210023, China*

Fax: +86-25-83243286; Tel: +86-25-85891651

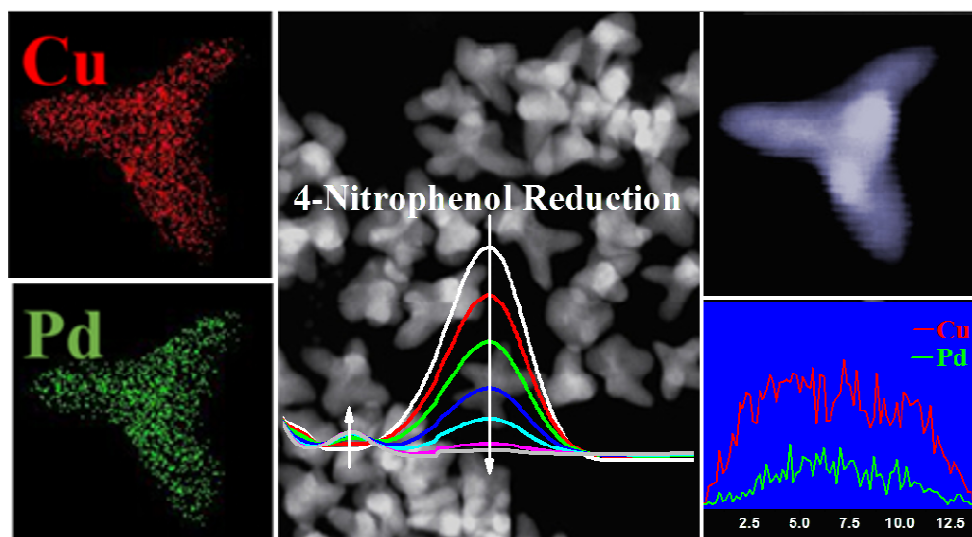
E-mail: tangyawen@njnu.edu.cn (Y. Tang);

weishaohua@njnu.edu.cn (S. Wei)

‡ Both authors contributed equally to this work

† Electronic Supplementary Information (ESI) available: Experimental Details. See DOI: 10.1039/c000000x/

- C. Hu, X. Zhai, Y. Zhao, K. Bian, J. Zhang, L. Qu, H. Zhang and H. Luo, *Nanoscale*, 2014, **6**, 2768-2775.
- J.-N. Zheng, L.-L. He, F.-Y. Chen, A.-J. Wang, M.-W. Xue and J.-J. Feng, *J. Mater. Chem. A*, 2014, **2**, 12899-12906.
- Z.-Y. Shih, C.-W. Wang, G. Xu and H.-T. Chang, *J. Mater. Chem. A*, 2013, **1**, 4773-4778.
- Y.-Y. Feng, G.-R. Zhang and B.-Q. Xu, *RSC Advances*, 2013, **3**, 1748-1752.
- W. Zhang, D. Cheng and J. Zhu, *RSC Advances*, 2014, **4**, 42554-42561.
- H. Kochkar, M. Aouine, A. Ghorbel and G. Berhault, *J. Phys. Chem. C*, 2011, **115**, 11364-11373.
- R. Zhao, G. Fu, T. Zhou, Y. Chen, X. Zhu, Y. Tang and T. Lu, *Nanoscale*, 2014, **6**, 2776-2781.
- W. Han, Z. Tang, P. Zhang and G. Lu, *RSC Advances*, 2014, **4**, 23262-23270.
- Z. Zhang, C. Zhang, J. Sun, T. Kou and C. Zhao, *RSC Advances*, 2012, **2**, 11820-11828.
- R. Wu, Q.-C. Kong, C. Fu, S.-Q. Lai, C. Ye, J.-Y. Liu, Y. Chen and J.-Q. Hu, *RSC Advances*, 2013, **3**, 12577-12580.
- Z. Yin, W. Zhou, Y. Gao, D. Ma, C. J. Kiely and X. Bao, *Chem-Eur. J.*, 2012, **18**, 4887-4893.
- D. Reyter, D. Bélanger and L. Roué, *The J. Phys. Chem. C*, 2008, **113**, 290-297.
- F. Fouda-Onana, S. Bah and O. Savadogo, *J. Electro. Chem.*, 2009, **636**, 1-9.
- K. H. Park, Y. W. Lee, S. W. Kang and S. W. Han, *Chem-Asian J.*, 2011, **6**, 1515-1519.
- S. Hu, L. Scudiero and S. Ha, *Electrochim. Acta.*, 2012, **83**, 354-358.
- J. Mao, Y. Liu, Z. Chen, D. Wang and Y. Li, *Chem. Commun.*, 2014, **50**, 4588-4591.
- A. M. McDonald, L. J. Cabri, N. S. Rudashevsky, C. J. Stanley, V. N. Rudashevsky and K. C. Ross, *The Canadian Mineralogist*, 2008, **46**, 709-716.
- G. Fu, K. Wu, X. Jiang, L. Tao, Y. Chen, J. Lin, Y. Zhou, S. Wei, Y. Tang, T. Lu and X. Xia, *Phys. Chem. Chem. Phys.*, 2013, **15**, 3793-3802.
- G. Fu, W. Han, L. Yang, J. Lin, S. Wei, Y. Chen, Y. Zhou, Y. Tang, T. Lu and X. Xia, *J. Mater. Chem.*, 2012, **22**, 17604-17611.
- T. Chierchie and C. Mayer, *Electrochim. Acta.*, 1988, **33**, 341-345.
- J. Okada, J. Inukai and K. Itaya, *Phys. Chem. Chem. Phys.*, 2001, **3**, 3297-3302.
- K. Lee, S. W. Kang, S.-U. Lee, K.-H. Park, Y. W. Lee and S. W. Han, *ACS Appl. Mater. Inter.*, 2012, **4**, 4208-4214.
- Z. Niu, D. Wang, R. Yu, Q. Peng and Y. Li, *Chem. Sci.*, 2012, **3**, 1925-1929.
- D. Wang, Q. Peng and Y. Li, *Nano Res.*, 2010, **3**, 574-580.
- D. Wang and Y. Li, *J. Am. Chem. Soc.*, 2010, **132**, 6280-6281.
- G. Fu, X. Jiang, L. Tao, Y. Chen, J. Lin, Y. Zhou, Y. Tang and T. Lu, *Langmuir*, 2013, **29**, 4413-4420.
- M. Gong, G. Fu, Y. Tang, Y. Chen and T. Lu, *ACS Appl. Mater. Interfaces*, 2014, **6**, 7301-7308.
- F. Wu and Q. Yang, *Nano Res.*, 2011, **4**, 861-869.
- J. Zhou and Q. Yang, *Chem-Asian J.*, 2012, **7**, 2045.
- F. Coccia, L. Tonucci, D. Bosco, M. Bressan and N. d'Alessandro, *Green Chem.*, 2012, **14**, 1073-1078.
- G. Fu, L. Ding, Y. Chen, J. Lin, Y. Tang and T. Lu, *CrystEngComm*, 2014, **16**, 1606-1610.



Bimetallic Pd<sub>1</sub>Cu<sub>3</sub> nanomultipods exhibited excellent catalytic activity for the 4-nitrophenol reduction.